| | |
|---|---|
| Title | Radiosensitivity of pimonidazole-unlabelled intratumour quiescent cell population to γ-rays, accelerated carbon ion beams and boron neutron capture reaction. |
| Author(s) | Masunaga, S; Sakurai, Y; Tanaka, H; Hirayama, R; Matsumoto, Y; Uzawa, A; Suzuki, M; Kondo, N; Narabayashi, M; Maruhashi, A; Ono, K |
| Citation | British journal of radiology (2013), 86 |
| Issue Date | 2013-01 |
| URL | http://hdl.handle.net/2433/174328 |
| Right | © 2013 The British Institute of Radiology |
| Type | Journal Article |
| Textversion | author |

# Radio-sensitivity of pimonidazole-unlabeled intratumor quiescent cell population to -rays, accelerated carbon ion beams and boron neutron capture reaction

[1]S MASUNAGA, MD, PhD, [2]Y SAKURAI, PhD, [2]H TANAKA, PhD, [3]R HIRAYAMA, PhD, [3]Y MATSUMOTO, PhD, [3]A UZAWA, PhD, [1]M SUZUKI, MD, PhD, [1]N KONDO, MD, PhD, [1]M NARABAYASHI, MD, PhD, [2]A MARUHASHI, PhD and [1]K ONO, MD, PhD

[1]*Particle Radiation Oncology Research Center and* [2]*Radiation Medical Physics, Research Reactor Institute, Kyoto University, Osaka, Japan.*

[3]*Research Center for Charged Particle Therapy, National Institute of Radiological Sciences, Chiba, Japan.*

**All correspondence to:**

Shin-ichiro Masunaga, M.D., Ph.D.
Particle Radiation Oncology Research Center,
Research Reactor Institute, Kyoto University,
2-1010, Asashiro-nichi, Kumatori-cho, Sennan-gun,
Osaka 590-0494, Japan.
Tel: +81-72-451-2406, 2487, Fax: +81-72-451-2627
E-mail: smasuna@rri.kyoto-u.ac.jp

# Radio-sensitivity of pimonidazole-unlabeled intratumor quiescent cell population to -rays, accelerated carbon ion beams and boron neutron capture reaction

**Abstarct**

Objectives: Detecting the radio-sensitivity of intratumor quiescent (Q) cells unlabeled with pimonidazole to accelerated carbon ion beams and the boron neutron capture reaction (BNCR).

Methods: EL4 tumor-bearing C57BL/J mice received 5-bromo-2′-deoxyuridine (BrdU) continuously to label all intratumor proliferating (P) cells. After the administration of pimonidazole, tumors were irradiated with -rays, accelerated carbon-ion beams, or reactor neutron beams with the prior administration of a $^{10}$B-carrier. Responses of intratumor Q and total (= P + Q) cell populations were assessed based on frequencies of micronucleation and apoptosis using immunofluorescence staining for BrdU. The response of pimonidazole-unlabeled tumor cells was assessed by means of apoptosis frequency using immunofluorescence staining for pimonidazole.

Results: Following -ray irradiation, the pimonidazole-unlabeled tumor cell fraction showed significantly enhanced radio-sensitivity compared with the whole tumor cell fraction more remarkably in the Q than total cell populations. However, a significantly greater decrease in radio-sensitivity in the pimonidazole-unlabeled cell fraction, evaluated using a delayed assay or a decrease in radiation dose rate, was more clearly observed among the Q than total cells. These changes in radio-sensitivity

were suppressed following carbon-ion beam and neutron beam only irradiaton. In BNCR, the use of a $^{10}$B-carrier, especially *L-para*-boronophenylalanine-$^{10}$B, enhanced the sensitivity of the pimonidazole-unlabeled cells more clearly in the Q than total cells.

Conclusions: The radio-sensitivity of the pimonidazole-unlabeled cell fraction depends on the quality of radiation delivered and characteristics of the $^{10}$B-carrier used in BNCR.

Advances in knowledge: The pimonidazole-unlabeled sub-fraction of Q tumor cells may be a critical target in tumor control.

**Keywords:**

quiescent cell; hypoxia;  -rays; carbon ion beam; boron neutron capture reaction; pimonidazole

**Authors have no conflict of interest concerning this manuscript.**

## Introduction

Human solid tumors are thought to contain moderately large fractions of quiescent (Q) tumor cells, which are not involved in the cell cycle and have stopped dividing, but which are as viable as established experimental animal tumor lines [1]. The presence of Q cells is probably due, at least in part, to hypoxia and the depletion of nutrition in the tumor core as a consequence of poor vascular supply [1]. As a result, with the exception of non-viable Q cells at the very edge of the necrotic rim where there is diffusion-limited hypoxia, Q cells are viable and clonogenic but have ceased dividing.

Using our method for selectively detecting the response of Q cells in solid tumors to treatment that damages DNA, the Q cell population in solid tumors has been shown to exhibit more resistance to conventional radio- and chemotherapy [2]. The Q cell population has also been demonstrated to have greater capacity to recover from radiation- and chemotherapeutic agent-induced damage and to have a significantly larger hypoxic fraction (HF) irrespective of the *p53* status of tumor cells [2]. However, the Q cell population in solid tumors has never been shown to be fully hypoxic [2]. Actually, the size of the HF of Q cell populations in SCC VII squamous cell carcinomas, implanted in the hind legs of C3H/He mice and with a diameter of 1 cm, was 55.1 ± 6.2 (mean ± SE) % [3]. Thus, this value was significantly less than 100 %, indicating that the Q cell population undoubtedly includes oxygenated tumor cells.

A few years ago, the universal detection of hypoxic cells in both tissues and cell cultures became possible using pimonidazole, a

substituted 2-nitroimidazole, and a mouse IgG1 monoclonal antibody (MAb1) to stable covalent adducts formed through reductive activation of pimonidazole in hypoxic cells [4]. Here, we tried to selectively detect the response of the pimonidazole-unlabeled and probably oxygenated cell fraction of the Q cell population. To achieve this we combined our method for selectively detecting the response of Q cells in solid tumors with the method for detecting cell and tissue hypoxia using pimonidazole and MAb1 to pimonidazole.

High-linear energy transfer (LET) radiation including neutrons is more effective [2] than low-LET X- or  -radiation at inducing biological damage. High-LET radiation shows a higher relative biological effectiveness (RBE) value for cell killing, a reduced oxygen effect, and a reduced dependence on the cell-cycle [2,5], making it potentially superior to low-LET radiation in the treatment of malignant tumors. Reactor thermal and epithermal neutron beams available at our institute had been also shown to have a significantly higher RBE value than  -rays in irradiated tumor cells *in vivo* [2]. Due to a selective physical dose distribution and enhanced biological damage in target tumors, particle radiation therapy with protons or heavy ions has gained increasing interest worldwide, and many clinical centers are considering introducing radiation therapy with charged particles. However, almost all reports on the biological advantages of charged particle beams are based on effects only on total tumor cell populations as a whole using *in vitro* cell cultures or *in vivo* solid tumors [1,5].

Intensity modulated radiotherapy and stereotactic irradiation

have become common as new radiotherapy modalities for the treatment of malignancies. These techniques often require precise positioning of patients and longer exposure times in a single treatment session [6, 7]. Prolongation of irradiation time may induce adverse radiation effects and evokes major concern related to the dose-rate effect. Thus, there is a need to clarify the effect of a reduction in dose-rate on the radio-sensitivity of tumors *in vivo*.

In the present study, the radio-sensitivity of the pimonidazole-unlabeled cell fraction of the Q cell population, following cobalt-60 -ray or 290 MeV/u accelerated carbon ion beam irradiation at both a high dose rate (HDR) and a reduced dose rate (RDR), was determined, compared with irradiation using reactor thermal neutron beams following the adminstration of a $^{10}$B-carrier at our institute. This is the first attempt to evaluate the sensitivity of oxygenated fractions of Q tumor cells *in vivo* in response to particle radiation.

## Methods

### *Mice and Tumors*

EL4 lymphoma cells (Cell Resource Center for the Biomedical Research Institute of Development, Aging and Cancer, Tohoku University) derived from C57BL/6J mice were maintained *in vitro* in RPMI 1640 medium supplemented with 12.5 % fetal bovine serum. The *p53* status of the EL4 tumor cells was the wild type [8]. Cells were collected from exponentially growing cultures and approximately $1.0 \times 10^5$ tumor cells were inoculated subcutaneously into the left hind legs of 9-week-old syngeneic female C57BL/6J mice (Japan Animal Co., Ltd., Osaka, Japan). Fourteen days after the inoculation, the tumors, approximately 1 cm in diameter, were employed for irradiation in this study, and the body weight of the tumor-bearing mice was 22.1 ± 2.3 g. Mice were handled according to the Recommendations for Handling of Laboratory Animals for Biomedical Research, compiled by the Committee on Safety Handling Regulations for Laboratory Animal Experiments.

### *Labeling with 5-bromo-2′-deoxyuridine (BrdU)*

Nine days after the tumor inoculation, mini-osmotic pumps (Durect Corporation, Cupertino, CA) containing BrdU dissolved in physiological saline (250 mg/ml) were implanted subcutaneously to enable the labeling of all P cells over a 5-day period [9]. The percentage of labeled cells after continuous labeling with BrdU was 66.1 ± 3.8 % and plateau at this stage. Therefore, tumor cells not incorporating BrdU after continuous exposure were regarded as Q cells.

### *Treatment*

After the labeling with BrdU, tumor-bearing mice received an intraperitoneal administration of pimonidazole hydrochloride

(Hypoxyprobe Inc., Burlington, MA, USA) dissolved in physiological saline at a dose of 60 mg/kg. Ninety minutes later, mice received -ray or accelerated carbon-ion beam irradiation, or reactor neutron beam irradiation following administration of the $^{10}$B-carrier with no anesthetic.

-Rays were delivered using a cobalt-60 -ray irradiator at dose rates of 2.5 and 0.039 Gy/min representing HDR and RDR irradiation, respectively. Carbon-12 ions were accelerated up to 290 MeV/u by the synchrotron of the Heavy Ion Medical Accelerator installed at the National Institute of Radiological Sciences in Chiba, Japan. The dose rate was regulated through a beam attenuation system, and irradiation was conducted using horizontal carbon beams with a dose rate of 1.0 or 0.035 Gy/min. The LET of a carbon ion beam with a 6-cm spread-out Bragg peak (SOBP) ranges from 14 keV/μm to greater than 200 keV/μm, depending on depth. The desired LET beam was obtained by selecting the depth along the beam path using a Lucite range shifter. An LET of 50 keV/μm at the middle of the SOBP was employed here.

Sodium mercaptoundecahydrododecaborate-$^{10}$B (sodium borocaptate-$^{10}$B, BSH, $Na_2{}^{10}B_{12}H_{11}SH$) (125 mg·kg$^{-1}$) and boronophenylalanine-$^{10}$B (BPA, $C_9H_{12}{}^{10}BNO_4$) (250 mg·kg$^{-1}$) were purchased from KatChem Ltd. (Czech Republic) and prepared freshly by dissolving in physiological saline and injected intraperitoneally in a volume of 0.02 mL·g$^{-1}$ mouse body weight. In accordance with our previous study [10], at a dose of less than 500 mg·kg$^{-1}$for BSH and less than 1,500 mg·kg$^{-1}$for BPA, no apparent toxicity was observed. Based on the certificate of analysis and Material Safety Data Sheet provided, BSH was not contaminated with the borocapatate dimer (BSSB, $[^{10}B_{24}H_{22}S_2]^{4-}$). Since the intratumor

$^{10}B$ concentration during neutron irradiation is a crucial determinant of the cell-kill effect in BNCR, to obtain similar intratumor $^{10}B$ concentrations during exposure to the neutron beam, irradiation was started at selected time points after the intraperitoneal injection of the $^{10}B$-carriers at a selected dose of $^{10}B$. Based on a preliminary study of the biodistribution of $^{10}B$, irradiation was started from 45 min after the intraperitoneal injection of 125 and 250 mg·kg$^{-1}$ (71.0 and 12.0 mg $^{10}B$·kg$^{-1}$) of BSH and BPA, respectively. $^{10}B$ concentrations were determined with a thermal neutron guide tube installed at the Kyoto University Research Reactor (KUR) [11].

The tumor-bearing mice were irradiated with a reactor neutron beam at a power of 1 MW at KUR. A LiF thermoplastic shield was employed to avoid irradiating other body parts except implanted solid tumors. Neutron irradiation was performed using a reactor neutron beam with a cadmium ratio of 9.4. The cadmium ratio is the ratio of the response of an uncovered neutron detector to that of the same detector under identical conditions when it is covered with cadmium of a specified thickness. The neutron fluence was measured from the radioactivation of gold foil at both the front and back of the tumors. Since the tumors were small and located just beneath the surface, the neutron fluence was assumed to decrease linearly from the front to back of the tumors. Thus, we used the average neutron fluence determined from the values measured at the front and back. Contaminating -raydosesincludingsecondary -rays were measured with a thermoluminescence dosimeter (TLD) powder at the back of the tumors. The TLD used was Beryllium Oxide (BeO) enclosed in a quartz glass capsule. BeO itself has some sensitivity to thermal neutrons. The thermal neutron fluence of 8 x $10^{12}$ cm$^{-2}$ is equal to

an approximately 1 cGy -ray dose. We usually use the TLD together with gold activation foil for the neutron-sensitivity correction. The details have been described previously [12]. For the estimation of neutron energy spectra, eight kinds of activation foil and fourteen kinds of nuclear reaction were used [12]. The absorbed dose was calculated using the flux-to-dose conversion factor [13]. The tumors contained H (10.7 % in terms of weight), C (12.1 %), N (2 %), O (71.4 %), and others (3.8 %) [14]. The average neutron flux and Kerma rate of the employed beam were 1.0 x $10^{9}$ n·cm$^{-2}$·s$^{-1}$ and 48.0 cGy·h$^{-1}$ for the thermal neutron range (less than 0.6 eV), 1.6 x $10^{8}$ n·cm$^{-2}$·s$^{-1}$and 4.6 cGy·h$^{-1}$ for the epithermal neutron range (0.6 through 10 keV), and 9.4 x $10^{6}$ n·cm$^{-2}$·s$^{-1}$and 32.0 cGy·h$^{-1}$ for the fast neutron range (more than 10 keV), respectively. The Kerma rate for boron dose per $\Phi$ n·cm$^{-2}$·s$^{-1}$ of thermal neutron flux for 1 μg·g$^{-1}$ of $^{10}$B was 2.67 x $10^{-8}$ $\Phi$ cGy·h$^{-1}$. The contaminating -ray dose rate was 66.0 cGy·h$^{-1}$.

Individual animals were secured in a specially designed device made of acrylic resin with the tail firmly fixed in position with adhesive tape. Each treatment group also included mice that had not been pretreated with BrdU.

***Immunofluorescence Staining of BrdU-Labeled and/or Pimonidazole-Labeled Cells and the Observation of Apoptosis and Micronucleation***

Based on our previous report related to the determination of the timing of apoptosis [10], as an immediate assay, an apoptosis assay was undertaken at 6 h after irradiation and a micronucleus assay was carried out immediately after irradiation. Tumors were excised from mice given BrdU, weighed, minced and trypsinized (0.05% trypsin and 0.02% ethylenediamine-tetraacetic acid (EDTA) in

phosphate-buffered saline (PBS) at 37 °C for 20 min). Furthermore, as a delayed assay, tumors were also excised from mice given BrdU, weighed, minced and trypsinized at 30 h after irradiation for the apoptosis assay, and at 24 h after irradiation for the micronucleus assay. For the apoptosis assay, single cell suspensions were fixed without further treatment. For the micronucleus assay, tumor cell suspensions were incubated for 72 h in tissue culture dishes containing complete culture medium and 1.0 μg/ml of cytochalasin-B, to inhibit cytokinesis while allowing nuclear division. The cultures were then trypsinized and cell suspensions were fixed. For both assays, after the centrifugation of fixed cell suspensions, the cell pellet was resuspended with cold Carnoy's fixative (ethanol:acetic acid = 3:1 in volume). The suspension was placed on a glass microscope slide and the sample was dried at room temperature. Slides were treated with 2 M hydrochloric acid for 60 min at room temperature to dissociate the histones and partially denature the DNA. They were then immersed in borax-borate buffer (pH 8.5) to neutralize the acid. BrdU-labeled tumor cells were detected using indirect immunofluorescence staining with a rat monoclonal anti-BrdU antibody (Abcam plc, Cambridge, UK) and a goat Alexa Fluor 488-conjugated anti-rat IgG antibody (Invitrogen Corp., Carlsbad, CA, USA). Pimonidazole-labeled tumor cells were detected using indirect immunofluorescence staining with a mouse monoclonal anti-pimonidazole antibody (Hypoxyprobe Inc., Burlington, MA, USA) and a rabbit Alexa Fluor 594-conjugated anti-mouse IgG antibody (Invitrogen Corp., Carlsbad, CA, USA). To enable the observation of the triple staining of tumor cells with green-emitting Alexa Fluor 488 and red-emitting Alexa Fluor 594, cells on the slides were treated with blue-emitting 4'6-diamidino-2-phenylindole

(DAPI) (0.5 µg/ml in PBS) and imaged using a fluorescence microscope.

The frequency of apoptosis in cells not labeled with BrdU (= Q cells at irradiation) and tumor cells not labeled with pimonidazole was determined by counting apoptotic cells in tumor cells that did not show green fluorescence from Alexa Fluor 488 and red fluorescence from Alexa Fluor 594, respectively. The apoptosis frequency was defined as the ratio of the number of apoptotic cells to the total number of observed tumor cells [10]. The micronucleus frequency in BrdU-unlabeled cells was examined by counting the micronuclei in the binuclear cells that did not show green fluorescence emitted by Alexa Fluor 488. The micronucleus frequency was defined as the ratio of the number of micronuclei in the binuclear cells to the total number of binuclear cells observed [2].

The ratios obtained in tumors not pretreated with BrdU indicated the apoptosis frequency and the micronucleus frequency in the total (P + Q) tumor cell populations. More than 300 tumor cells and binuclear cells were counted to determine the apoptosis frequency and the micronucleus frequency, respectively.

***Clonogenic Cell Survival Assay***

The clonogenic cell survival assay was also performed in mice given no BrdU or pimonidazole using an *in vivo-in vitro* assay method. Tumors were disaggregated by stirring for 20 min at 37 °C in PBS containing 0.05 % trypsin and 0.02% EDTA. The cell yield was (1.1 ± 0.3) x $10^8$/g tumor weight. A colony formation assay using the *in vivo-in vitro* assay method was performed with the culture medium mixed with methylcellulose (15.0 g/L) (Aldrich, Milwaukee, WI, USA).

The apoptosis and micronucleus frequencies and surviving fractions for the total cell population were obtained from cells in tumors that were not pretreated with BrdU or pimonidazole. The apoptosis and micronucleus frequencies for Q cells were obtained from unlabeled tumor cells after continuous BrdU labeling without pimonidazole loading. The apoptosis frequencies for the total tumor cell populations that were not labeled with pimonidazole were obtained from tumor cells that were not labeled with pimonidazole after pimonidazole loading without BrdU pretreatment. The apoptosis frequencies for Q cells that were not labeled with pimonidazole were obtained from tumor cells that were not labeled with BrdU or pimonidazole after both continuous BrdU labeling and pimonidazole loading. Thus, there was no effect of interaction between BrdU and irradiation or between pimonidazole and irradiation on the values for the apoptosis and micronucleus frequencies and surviving fractions. Incidentally, since the rate of pimonidazole-labeled tumor cells could change during culturing with cytochalasin-B over 3 days, following the production of single tumor cell suspensions by excising and mincing the tumors from mice that underwent pimonidazole loading, the micronucleus frequency for the cell fraction that was not labeled with pimonidazole after pimonidazole loading was not determined. As a consequence, the radiosensitivity of the pimonidazole-unlabeled cell fractions was only determined in relation to apoptosis induction. This was the reason for using the EL4 leukemia cell line with its much greater capacity for the induction of apoptosis than other solid tumor-originating cell lines [10].

***Data Analysis and Statistics***

More than three tumor-bearing mice were used to assess each set

of conditions and each experiment was repeated at least twice. To examine the differences between pairs of values, Student's *t*-test was used when variances of the two groups were assumed to be equal with Shapiro-Wilk normality test; otherwise the Welch *t*-test was used.

**Results**

The plating efficiency and the micronucleus and apoptosis frequencies after a radiation dose of 0 Gy are shown in **Table 1**. The micronucleus and apoptosis frequencies were significantly higher for the Q cell population than for the total cell population. In contrast, the apoptosis frequency was significantly lower for the cell fraction that was not labeled with pimonidazole than for the whole tumor cell fraction in both the Q and total tumor cell populations.

Cell survival curves for the total tumor cell population as a function of radiation dose are shown in **Figure 1**. In the irradiation of -rays and carbon-ion beams, the surviving fractions (SFs) increased in the following order with a more remarkable change for -rays than carbon-ion beams: immediately after HDR irradiation < 24 h after HDR irradiation < immediately after RDR irradiation. In BNCR, the SFs increased in the following order: with BPA < with BSH < without a $^{10}$B-carrier.

For baseline correction, we used the net micronucleus frequency to exclude the micronucleus frequency in non-irradiated tumors. The net micronucleus frequency was defined as the micronucleus frequency in the irradiated tumors minus the micronucleus frequency in the non-irradiated tumors. Dose response curves for the net micronucleus frequency in total and Q tumor cell populations as a function of radiation dose are shown in **Figure 2**. Overall, the net micronucleus frequencies were significantly lower in the Q cells than the total cell population. In both the total and Q cell populations after the irradiation of -rays and carbon-ion beams, the net micronucleus frequencies decreased in the following order with a more remarkable change for -rays than carbon-ion beams:

immediately after HDR irradiation > 24 hours after HDR irradiation > immediately after RDR irradiation. In BNCR, the net micronucleus frequencies for the total cell population increased in the following order: without a $^{10}$B-carrier < with BSH < with BPA. However, those for the Q cell population increased in the following order: without a $^{10}$B-carrier < with BPA < with BSH.

For another baseline correction, we used the net apoptosis frequency to exclude the apoptosis frequency in non-irradiated tumors. The net apoptosis frequency was the apoptosis frequency in the irradiated tumors minus that in the non-irradiated tumors. Dose response curves for the net apoptosis frequency in the total and Q tumor cell populations as a function of radiation dose are shown in **Figure 3**. Overall, the net apoptosis frequencies were significantly lower in the Q than total cell population, with much larger differences for -rays than carbon-ion beams. Moreover, the net apoptosis frequency was significantly higher for the cell fraction that was not labeled with pimonidazole than for the whole tumor cell fraction in both the Q and total cell populations under each set of conditions, again with a much larger difference for -rays than carbon-ion beams. For both the pimonidazole-unlabeled and the whole cell fractions, in the Q as well as total tumor cell population, the net apoptosis frequencies decreased in the following order with a more remarkable change for -rays than carbon-ion beams: immediately after HDR irradiation > 24 h after HDR irradiation > immediately after RDR irradiation. Also in BNCR, the pimonidazole-unlabeled cells showed higher net apoptosis frequencies than the whole tumor cell fractions with little remarkable change in the Q compared to total cell population and with increased change in the following order: without a $^{10}$B-carrier

< with BSH < with BPA.

To evaluate the radio-sensitivity of the cell fraction that was not labeled with pimonidazole, as compared with the whole cell fraction in both the total and Q cell populations, dose-modifying factors (DMFs) were calculated using the data obtained under -ray and carbon-ion beam irradiation conditions (**Fig. 3**, **Table 2**). Overall, DMF values tended to be higher for the Q cell than total cell population, and in particular immediately after HDR irradiation with a much larger difference for -rays than carbon-ion beams. In the total cell population, the DMF values were almost constant. However, for Q cells, the DMF values had a tendency to decrease in the following order: immediately after HDR irradiation > 24 h after HDR irradiation > immediately after RDR irradiation. Also in BNCR (**Table 3**), DMF values tended to be higher for the Q cell than total cell population, and in both Q and Total cell populations, the DMF values had a tendency to increase in the following order: without a $^{10}$B-carrier < with BSH < with BPA.

To investigate the reduction in radio-sensitivity caused by a delayed assay or a decrease in the radiation dose rate, DMFs were calculated using the data for -ray and carbon-ion beam irradiation conditions given in **Figures 1** through **3** (**Table 4**). Overall, carbon beams showed lower DMF values than -rays under all sets of conditions. On the whole, in the fraction unlabeled with pimonidazole or the whole cell fraction, the values were higher after RDR irradiation than at 24 h after HDR irradiation in both the total and Q cell populations, particularly in the latter population. The DMF values were significantly higher in the Q cell than total cell population in both the pimonidazole-unlabeled and whole cell fractions. In both the Q and total cell populations,

the values were higher for pimonidazole-unlabeled cell fractions than whole cell fractions, particularly in the case of the Q cells.

To estimate the radio-enhancing effect of $^{10}$B-carriers, irradiation with BPA and BSH in the total and Q cell populations was compared with neutron beam irradiation only, using the data shown in **Figures 1** through **3** (**Table 5**). Both BPA and BSH enhanced the sensitivity of the total cell population significantly more than that of the Q cell population. Further, BPA tended to affect the total cell population more than did BSH. In contrast, the sensitivity of Q cells was relatively more enhanced with BSH than BPA. In both the Q and total cell populations but especially in Q cells, the values were higher for pimonidazole-unlabeled cell fractions than whole cell fractions.

To examine the difference in radio-sensitivity between the total and Q cell populations, DMFs that allow us to compare the dose of radiation necessary to obtain each end-point in the two cell populations, were calculated using the data in **Figures 2** and **3** (**Tables 6** and **7**). All DMF values were significantly higher than 1.0, and carbon beams showed smaller values than  -rays under each set of conditions (**Table 6**). The DMF values increased in the following order: immediately after HDR irradiation < 24 h after HDR irradiation < immediately after RDR irradiation. The values were lower for the sub-population that was not labeled with pimonidazole as compared with the whole cell population (**Table 6**). In BNCR, the DMF values increased in the following order: without $^{10}$B-carrier < with BSH < with BPA (**Table 7**). Again, the values were lower for the sub-population not labeled with pimonidazole than the whole cell population.

## Discussion

In recent years the concept of cancer stem cells (CSCs), or tumor-initiating cells (tumor clonogens), has attracted a great deal of interest because of the potential clinical significance [15]. In part, these cells are thought to exist in a pathophysiological microenvironment where hypoxia, low pH and nutrient deprivation occur. Under these microenvironmental conditions, dividing tumor cells have also been thought to become quiescent. Actually, a subset of CSCs or tumor clonogens consists of non-dividing quiescent cells [16]. Thus, in the current study we tried to clarify the radiobiological characteristics of the sub-population in the intratumor Q cell population in the context of CSC or tumor clonogen characteristices.

The fraction of cells that were not labeled with pimonidazole showed significantly higher radio-sensitivity than the whole cell fraction in both the Q and total cell populations, and amongst the Q cells in particular (**Table 2**). This was probably because the pimonidazole-unlabeled cells were more oxygenated than the whole cell fraction, which comprised oxygenated and hypoxic tumor cells, in both the Q and total tumor cell populations [4]. Additionally the Q cell population as a whole included a larger HF than the total tumor cell population [2]. As shown in **Table 4**, the pimonidazole-unlabeled cell fraction had a greater recovery capacity than the whole cell fraction, especially in the case of the Q cells. The radio-sensitivity decreased in the following order: immediately after HDR irradiation, at 24 h after HDR irradiation and immediately after RDR irradiation, particularly in the Q cells (**Table 4**). As a consequence, in the case of the Q cells, the difference in radio-sensitivity between the

pimonidazole-unlabeled and whole cell fractions declined in the same order (**Table 2**). One mechanism of CSC or tumor clonogen resistance to cytotoxic treatment is supposed to be based on an enhanced DNA repair capacity [17]. Here, the pimonidazole-unlabeled Q cell fraction showed a much greater recovery capacity than the Q cell population as a whole, even if the recovery capacity was significantly greater in the entire Q cell population than in the total tumor cell population as a whole. In other words, from the viewpoint of not only quiescent status but also enhanced DNA repair capacity, the characteristics of the pimonidazole-unlabeled cell fraction in the Q cell population were found to be similar to those of CSCs or tumor clonogens.

The microenvironmental conditions under which dividing tumor cells become quiescent might promote the formation of micronuclei and apoptosis at 0 Gy in the whole Q tumor cell fractions, partly due to hypoxic stress (**Table 1**) [1]. In this study, the Q cells were shown to be significantly less radiosensitive and to have a greater recovery capacity than the total cell population (**Figs. 2** and **3, Table 6**). This finding indicated that more Q cells survive radiation therapy than P cells. In particular, in the cell fraction that was not labeled with pimonidazole, the difference in radio-sensitivity between the Q and total cell populations was markedly increased when evaluated using the delayed assay or by employing a reduced radiation dose-rate. This was due to the greater recovery capacity of the unlabeled Q cell fraction as compared with the unlabeled cell fraction in the total tumor cell population (**Table 6**). Therefore, whether in the pimonidazole-unlabeled or the whole Q cell population, it follows that control of the Q cells has a great impact on the outcome of radiation therapy and that

the Q cell population can be a critical target in the control of solid tumors.

At high LET carbon ion irradiation, tumor radio-sensitivity and the capacity to recover from radiation-induced damage are known to be significantly less dependent on intratumor oxygenation status and the irradiation dose rate [18]. This is thought to be partly because the frequency of closely spaced DNA lesions forming a cluster of DNA damage produced by high LET carbon-ion beams is much less dependent on oxygenation status at the time of irradiation than that of DNA damage produced by low LET -ray irradiation [5, 18]. Thus, the differences in radio-sensitivity not only between total and Q cell populations but also between pimonidazole-unlabeled cells and the whole cell fraction in both the Q and total cell populations were efficiently reduced. Moreover, the capacity to recover from radiation-induced damage in both the Q and total cell populations as a whole and both the pimonidazole-unlabeled and the whole cell fraction of the Q and total cell populations was remarkably reduced (**Table 2** and **4**). These findings including newly elucidated characteristics concerning the response of the Q cell population and pimonidazole-unlabeled cell fraction in the total and Q cell pouplations potentially reveal some reliable advantage of high LET radiation over low LET radiation in terms of controlling the CSCs or tumor clonogens that are thought to be resistant to cytotoxic treatment for solid tumors.

In boron neutron capture therapy (BNCT), the cellular distribution of $^{10}B$ from BSH is thought mostly dependent on the diffusion of the drug, whereas that from BPA is more dependent on the ability of the cells to take up $^{10}B$ [19]. Further, Q cell populations have been shown to have a much larger HF than total

cell populations [2], and hypoxic cells are thought to exhibit less uptake ability than aerobic cells [1]. Therefore, it follows that Q cells have a lower uptake capacity than the total cell population, and that the distribution of $^{10}$B from $^{10}$B-carriers into Q cells is more dependent on the diffusion of the drugs than on the uptake ability of the cells. **Tables 3** and **5** show that the distribution of $^{10}$B in the tumor from BSH relies mostly on passive diffusion, whereas that from BPA relies on uptake capacity in tumor via active transport, the former resulting from a greater effect on Q cells, and the latter, that on the pimonidazole-unlabeled cell fraction and the total tumor cell population. In BNCR, when a $^{10}$B-carrier, especially BPA, is employed, the difference in radio-sensitivity not only between total and Q cell populations as a whole but also between pimonidazole-unlabeled cells and the whole cell fraction of the Q and total cell populations is rather extended compared with the case of disuse of $^{10}$B-carrier. Consequently, without a reliable method of delivering enough amount of $^{10}$B into target tumor cells efficiently irrespective of intratumor microenvironmental conditions including oxygenation status, it is hard to conclude that BNCT in combination with a $^{10}$B-carrier can overcome the resistance to cytotoxic treatment of CSCs or tumor clonogens. Also in BNCT, compared with reactor neutron beam irradiation only, Q cells have been shown to have significantly less radiosensitivity than the total cell population when a $^{10}$B-carrier, especially BPA, is employed (**Table 7**) [1,2,20]. Thus, more Q cells can survive BNCT than P cells (**Figs. 2** and **3**, **Table 7**).

In the present study, the pimonidazole-unlabeled, and probably oxygenated, cell fraction showed a greater recovery capacity than the Q cell population as a whole. However, although there is

similarity between the pimonidazole-unlabeled Q cell fraction and CSCs or tumor clonogens in terms of quiescent status and enhanced recovery capacity, CSCs or tumor clonogens are thought to exist under rather hypoxic conditions [15,16,17]. In the future, using human tumor cell lines, the characteristics of the intratumor Q cell population in connection with those of CSCs or tumor clonogens also have to be analyzed.

**Acknowledgments**

This study was supported in part by a Grant-in-aid for Scientific Research (B) (23300348, 23390355) from the Japan Society for the Promotion of Science.

**References**

1. Vaupel P. Tumor microenvironmental physiology and its implications for radiation oncology. Semin Radiat Oncol 2004;206:198-206.
2. Masunaga S, Ono K. Significance of the response of quiescent cell populations within solid tumors in cancer therapy. J Radiat Res 2002;43:11-25.
3. Masunaga S, Ono K, Suzuki M, Kinashi Y, Takagaki M. Radiobiologic significance of apoptosis and micronucleation in quiescent cells within solid tumors following -ray irradiation. Int J Radiat Oncol Biol Phys 2001;49:1361-1368.
4. Ljungkvist,AS, Bussink J, Rijken PF, Raleigh JA, Denekamp J, Van Der Kogel AJ. Changes in tumor hypoxia measured with a double hypoxic marker technique. Int J Radiat Oncol Biol Phys 2000;48:1529-1538.
5. Hada M, Georgakilas AG. Formation of clustered DNA damage after high-LET irradiation: a Review. J Radiat Res 2008;49:203-210.
6. Ahmed RS, Kim RY, Duan J, Meleth S, De Los Santos JF, Fiveash JB. IMRT dose escalation for positive para-aortic lymph nodes in patients with locally advanced cervical cancer while reducing dose to bone marrow and other organs at risk. Int J Radiat Oncol Biol Phys 2004;60:505-512.
7. Wulf J, Haedinger U, Oppitz U, Thiele W, Mueller G, Flentje M. Stereotactic radiotherapy for primary lung cancer and pulmonary metastases: a noninvasive treatment approach in medically inoperable patients. Int J Radiat Oncol Biol Phys 2004;60:186-196.
8. Masunaga S, Ono K, Suzuki M, Nishimura Y, Kinashi Y, Takagaki M, et al. Radiosensitization effect by combination with

paclitaxel *in vivo* including the effect on intratumor quiescent cells. Int J Radiat Oncol Biol Phys 2001;50:1063-1072.

9. Hall EJ, Giaccia AJ. Radiosensitivity and cell age in the mitotic cycle. In: Hall EJ, Giaccia AJ, editors. Radiobiology for the radiologist. 7th edition. Philadelphia, USA: Lippincott Williams & Wilkins, 2012: 54-66.
10. Masunaga S, Ono K, Sakurai Y, Takagaki M, Kobayashi T, Kinashi Y, et al. Evaluation of apoptosis and micronucleation induced by reactor neutron beams with two different cadmium ratios in total and quiescent cell populations within solid tumors. Int J Radiat Oncol Biol Phys 2001;51:828-839.
11. Kobayashi T, Kanda K. Microanalysis system of ppm-order $^{10}B$ concentrations in tissue for neutron capture therapy by prompt $\gamma$-ray spectrometry. Nucl Instrum Methods 1983;204:525-531.
12. Sakurai Y, Kobayashi T. Characteristics of the KUR Heavy Water Neutron Irradiation Facility as a neutron irradiation field with variable energy spectra. Nucl Instr Meth A 2000;453:569-596.
13. Kobayashi T, Sakurai Y, Kanda K, Fujita Y, Ono K. The remodeling and basic characteristics of the heavy water neutron irradiation facility of the Kyoto University Research Reactor, mainly for neutron capture therapy. Nucl Tech 2000;131:354-378.
14. Snyder WS, Cook MJ, Nasset ES, Karhausen LR, Parry Howells G, Tipton I. Gross and elemental content of reference man. In: Snyder WS (ed). Report of the task group on reference man. Oxford, UK: Pergamon Press, 1975:273–324.
15. O'Brien CA, Kreso A, Dick JE. Cancer stem cells in solid tumors: an overview. Semin Radiat Oncol 2009;19:71-76.
16. Hill RP, Marie-Egyptienne DT, Hedley DW. Cancer stem cells,

hypoxia and metastasis. Semin Radiat Oncol 2009;19:106-111.

17. Diehn M, Cho RW, Clarke MF. Therapeutic implications of the cancer stem cell hypothesis. Semin Radiat Oncol 2009;19:78-85.
18. Hamada N, Imaoka T, Masunaga S, Ogata T, Okayasu R, Takahashi A, et al. Recent advances in the biology of heavy-ion cancer therapy. J Radiat Res 2010;51:365-383.
19. Soloway AH, Hatanaka H, Davis MA. Penetration of brain and brain tumor. VII. Tumor-binding Sulfhydryl Boron Compounds. J Med Chem 1967;10:714-717.
20. Vaupel P, Kallinowski F, Okunieff P. Blood flow, oxygen and nutrient supply, and metabolic microenvironment of human tumors: a review. Cancer Res 1989;49:6449-6465.

**Figure legends**

**Figure 1.** Cell survival curves for the whole tumor cell fraction in the total tumor cell population of EL4 tumors as a function of -ray (a), accelerated carbon ion beam (b) or reactor neutron beam (c) radiation dose. Circles, triangles and squares represent the surviving fractions immediately after (HDR) and at 24 h after (Delayed) high dose-rate and reduced dose-rate (RDR) -ray or accelerated carbon ion beam irradiation, respectively. For reactor neutron beam irradiation, circles, triangles and squares represent the surviving fractions for without a $^{10}$B-carrier (Boron (-)), with boronophenylalanine-$^{10}$B (BPA), and with sodium mercaptoundecahydrododecaborate-$^{10}$B (BSH), respectively. Bars represent standard errors (n = 9).

**Figure 2.** Dose response curves of the net micronucleus frequency for the whole tumor cell fraction in the total and quiescent (Q) tumor cell populations of EL4 tumors as a function of -ray (a), accelerated carbon ion beam (b) or reactor neutron beam (c) radiation dose. Open and solid symbols represent the net micronucleus frequencies for total and quiescent tumor cell populations, respectively. Circles, triangles and squares represent the net micronucleus frequencies immediately after (HDR) and at 24 h after (Delayed) high dose-rate and reduced dose-rate (RDR) -ray or accelerated carbon ion beam irradiation, respectively. For reactor neutron beam irradiation, circles, triangles and squares represent the net micronucleus frequencies for without a $^{10}$B-carrier (Boron

(-)), with boronophenylalanine-$^{10}$B (BPA), and with sodium mercaptoundecahydrododecaborate-$^{10}$B (BSH), respectively. Bars represent standard errors (n = 9).

**Figure 3.** Dose response curves for the net apoptosis frequency of the total (left panel) and quiescent (Q) (right panel) tumor cell populations of EL4 tumors as a function of -ray (a), accelerated carbon ion beam (b) or reactor neutron beam (c) radiation dose. Open and solid symbols represent the net apoptosis frequencies for the whole tumor cell fraction and the cell fraction not labeled with pimonidazole (Pimo (-)) in both the total and Q tumor cell populations, respectively. Circles, triangles and squares represent the net apoptosis frequencies immediately after (HDR) and at 24 h after (Delayed) high dose-rate and reduced dose-rate (RDR) -ray or accelerated carbon ion beam irradiation, respectively. For reactor neutron beam irradiation, circles, triangles and squares represent the net apoptosis frequencies for without a $^{10}$B-carrier (Boron (-)), with boronophenylalanine-$^{10}$B (BPA), and with sodium mercaptoundecahydrododecaborate-$^{10}$B (BSH), respectively. Bars represent standard errors (n = 9).

**Table 1.**

**Plating efficiency and micronucleus frequency at 0 Gy.**

| | Total tumor cells | Quiescent cells |
|---|---|---|
| **<Plating efficiency (%)>** | | |
| | **25.5 ± 6.8[a]** | **----** |
| **<Micronucleus frequency>** | | |
| | **0.053 ± 0.003** | **0.073 ± 0.006** |
| **<Apoptosis frequency>** | | |
| **In whole cell fraction** | | |
| | **0.040 ± 0.001** | **0.067 ± 0.004** |
| **In pimonidazole unlabeled cell fraction** | | |
| | **0.017 ± 0.001** | **0.028 ± 0.003** |

[a]; Mean ± standard error (n = 9)

**Table 2.**

**Dose-modifying factors for the pimonidazole unlabeled cell fraction as compared with the whole cell fraction in the total or quiescent cell population[a].**

| | High dose-rate Immediately after | High dose-rate 24 hours after | Reduced dose-rate |
|---|---|---|---|
| **<Net apoptosis frequency = 0.06>** | | | |
| **-Rays** | | | |
| **Total cell population** | | | |
| | **1.55 (1.45-1.65)[b]** | **1.5 (1.4-1.6)** | **1.5 (1.4-1.6)** |
| **Quiescent cell population** | | | |
| | **1.7 (1.5-1.9)** | **1.65 (1.55-1.75)** | **1.6 (1.5-1.7)** |
| **Carbon beams** | | | |
| **Total cell population** | | | |
| | **1.25 (1.1-1.4)** | **1.2 (1.1-1.3)** | **1.2 (1.1-1.3)** |
| **Quiescent cell population** | | | |
| | **1.6 (1.5-1.7)** | **1.5 (1.4-1.6)** | **1.4 (1.3-1.5)** |

[a]; The ratio of the dose of radiation necessary to obtain each end-point in a whole cell fraction to that needed to obtain each end-point in the pimonidazole unlabeled cell fraction.

[b]; Values in parentheses are 95% confidence limits, determined using standard errors. When the ranges of 95 % confidence limits showed no overlap between two values, the difference between the two values were significant *($p < 0.05$)* based on a Chi-squared test.

**Table 3.**

**Dose-modifying factors for the pimonidazole unlabeled cell fraction as compared with the whole cell fraction in the total or quiescent cell population[a].**

| Neutrons only | With BPA | With BSH |
|---|---|---|
| **<Net apoptosis frequency = 0.06>** | | |
| **Neutron beams** | | |
| **Total cell population** | | |
| **1.1 (1.0-1.2)[b]** | **1.3 (1.2-1.4)** | **1.25 (1.15-1.35)** |
| **Quiescent cell population** | | |
| **1.15 (1.05-1.25)** | **1.45 (1.3-1.6)** | **1.35 (1.25-1.45)** |

[a]; The ratio of the dose of radiation necessary to obtain each end-point in a whole cell fraction to that needed to obtain each end-point in the pimonidazole unlabeled cell fraction.

[b]; As in Table 2.

**Table 4.**

**Dose-modifying factors obtained using a delayed assay or a reduced radiation dose-rate[a].**

| | High dose-rate 24 hours after | Reduced dose-rate |
|---|---|---|
| **<Surviving fraction = 0.08>** | | |
| **Total cells** | | |
| **-Rays** | **1.15 (1.1-1.2)[b]** | **1.4 (1.3-1.5)** |
| **Carbon beams** | **1.1 (1.0-1.2)** | **1.2 (1.1-1.3)** |
| **<Net micronucleus frequency = 0.2>** | | |
| **Total cells** | | |
| **-Rays** | **1.2 (1.1-1.3)** | **1.35 (1.25-1.45)** |
| **Carbon beams** | **1.05 (1.0-1.1)** | **1.2 (1.1-1.3)** |
| **Quiescent cells** | | |
| **-Rays** | **1.4 (1.3-1.5)** | **1.6 (1.45-1.75)** |
| **Carbon beams** | **1.1 (1.0-1.2)** | **1.25 (1.15-1.35)** |
| **<Net apoptosis frequency = 0.06>** | | |
| **Total cells** | | |
| **In whole cell fraction** | | |
| **-Rays** | **1.15 (1.1-1.2)** | **1.3 (1.2-1.4)** |
| **Carbon beams** | **1.05 (1.0-1.2)** | **1.2 (1.1-1.3)** |
| **In pimonidazole unlabeled cell fraction** | | |
| **-Rays** | **1.2 (1.1-1.3)** | **1.3 (1.2-1.4)** |
| **Carbon beams** | **1.05 (1.0-1.2)** | **1.2 (1.1-1.3)** |
| **Quiescent cells** | | |
| **In whole cell fraction** | | |
| **-Rays** | **1.35 (1.25-1.45)** | **1.55 (1.45-1.65)** |
| **Carbon beams** | **1.15 (1.1-1.2)** | **1.25 (1.15-1.35)** |
| **In pimonidazole unlabeled cell fraction** | | |
| **-Rays** | **1.45 (1.35-1.55)** | **1.65(1.5-1.8)** |
| **Carbon beams** | **1.15 (1.1-1.2)** | **1.35(1.25-1.45)** |

[a]; The ratio of the dose of radiation necessary to obtain each end-point with a delayed assay or reduced dose-rate irradiation to that needed to obtain each end-point with an assay immediately after high dose-rate irradiation.

[b]; As in Table 2.

**Table 5.**

**Enhancement ratios[a] due to combination with a $^{10}$B-carrier**

| $^{10}$B-carrier | Total cell population | Quiescent cells |
|---|---|---|
| **<Surviving fraction = 0.08>** | | |
| **BPA[c]** | **1.95 (1.75-2.15)[b]** | **----** |
| **BSH[d]** | **1.3 (1.2-1.4)** | **----** |
| **<Net micronucleus frequency = 0.2>** | | |
| **BPA** | **2.0 (1.8-2.2)** | **1.7 (1.6-1.8)** |
| **BSH** | **1.3 (1.2-1.4)** | **1.8 (1.65-1.95)** |
| **<Net apoptosis frequency = 0.06>** | | |
| **In whole cell fraction** | | |
| **BPA** | **1.5 (1.4-1.6)** | **1.25 (1.15-1.35)** |
| **BSH** | **1.4 (1.3-1.5)** | **1.35 (1.2-1.5)** |
| **In pimonidazole unlabeled cell fraction** | | |
| **BPA** | **1.65 (1.5-1.8)** | **1.65 (1.5-1.8)** |
| **BSH** | **1.5 (1.4-1.6)** | **1.7 (1.6-1.8)** |

[a]; The ratio of the dose of radiation necessary to obtain each end-point without a $^{10}$B-carrier to that needed to obtain each end-point with a $^{10}$B-carrier.

[b]; As in Table 2.

[c]; *L-para*-boronophenylalanine-$^{10}$B

[d]; Sodium mercaptoundecahydrododecaborate-$^{10}$B

**Table 6.**

**Dose-modifying factors for quiescent cells relative to total tumor cells[a].**

| | High dose-rate immediately after | High dose-rate 24 hours after | Reduced dose-rate |
|---|---|---|---|
| **<Net micronucleus frequency = 0.2>** | | | |
| **-Rays** | | | |
| | **1.65 (1.5-1.8)[b]** | **1.8 (1.65-1.95)** | **1.9 (1.75-2.05)** |
| **Carbon beams** | | | |
| | **1.35 (1.25-1.45)** | **1.4 (1.25-1.55)** | **1.45 (1.3-1.6)** |
| **<Net apoptosis frequency = 0.06>** | | | |
| **In whole cell fraction** | | | |
| **-Rays** | | | |
| | **1.3 (1.2-1.4)** | **1.45 (1.35-1.55)** | **1.55 (1.4-1.7)** |
| **Carbon beams** | | | |
| | **1.15 (1.05-1.25)** | **1.25 (1.15-1.35)** | **1.3 (1.2-1.4)** |
| **In pimonidazole unlabeled cell fraction** | | | |
| **-Rays** | | | |
| | **1.2 (1.1-1.3)** | **1.4 (1.3-1.5)** | **1.55 (1.4-1.7)** |
| **Carbon beams** | | | |
| | **1.1 (1.0-1.2)** | **1.2 (1.1-1.3)** | **1.25 (1.15-1.35)** |

[a]; The ratio of the dose of radiation necessary to obtain each end-point in the quiescent cell population to that needed to obtain each end-point in the total tumor cell population.

[b]; As in Table 2.

**Table 7.**

**Dose-modifying factors for quiescent cells relative to total tumor cells[a].**

| Neutrons only | With BPA | With BSH |
|---|---|---|
| **<Net micronucleus frequency = 0.2>** | | |
| **1.2 (1.1-1.3)[b]** | **2.15 (1.9-2.4)** | **1.25 (1.15-1.35)** |
| **<Net apoptosis frequency = 0.06>** | | |
| **In whole cell fraction** | | |
| **1.3 (1.2-1.4)** | **1.6 (1.45-1.75)** | **1.25 (1.15-1.35)** |
| **In pimonidazole unlabeled cell fraction** | | |
| **1.25 (1.15-1.35)** | **1.35 (1.2-1.5)** | **1.15 (1.05-1.25)** |

[a]; The ratio of the dose of radiation necessary to obtain each end-point in the quiescent cell population to that needed to obtain each end-point in the total tumor cell population.

[b]; As in Table 2.

Figure 1
Click here to dOVYnload high resolution image

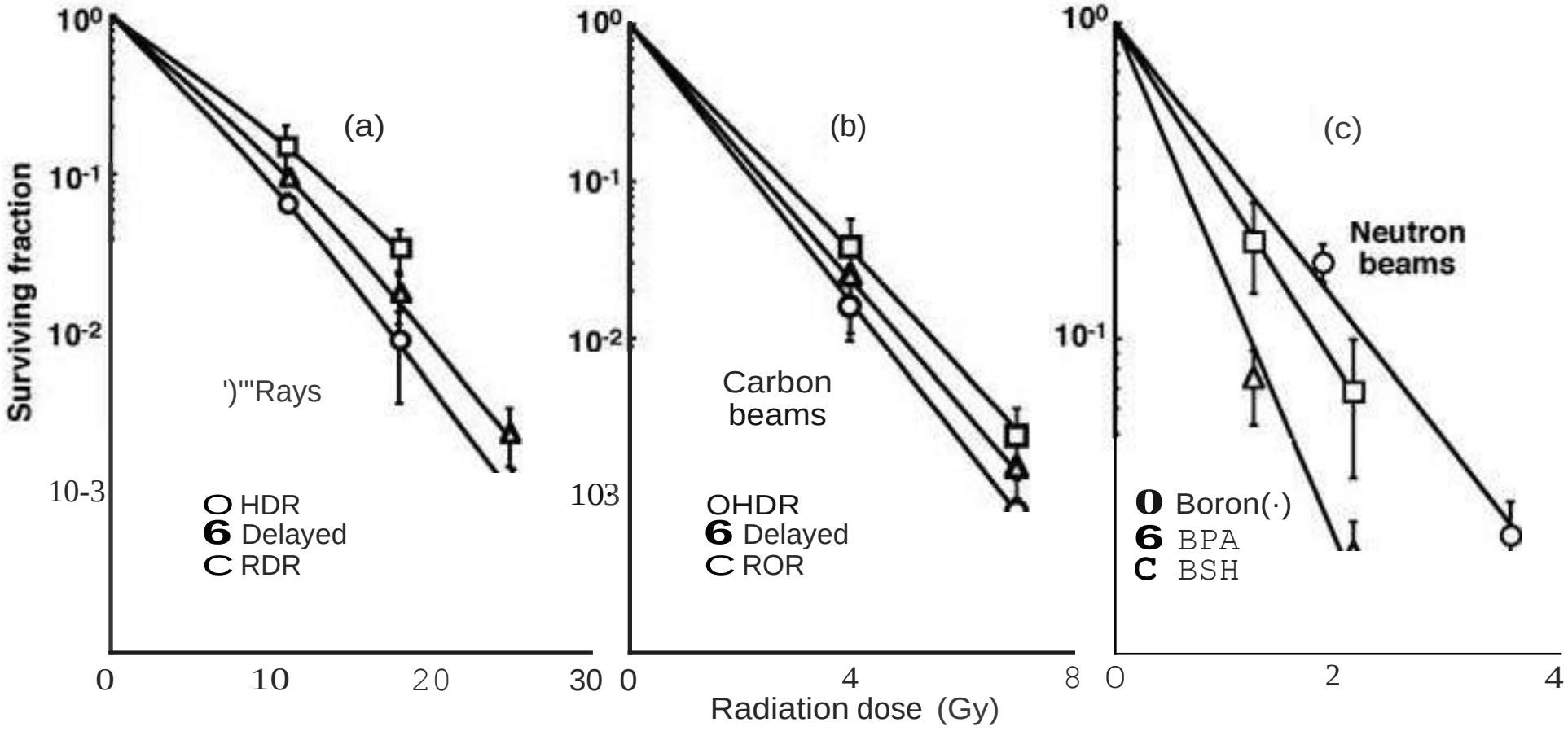

Figure 2
Click here to dcwvnb-d high resdlution image

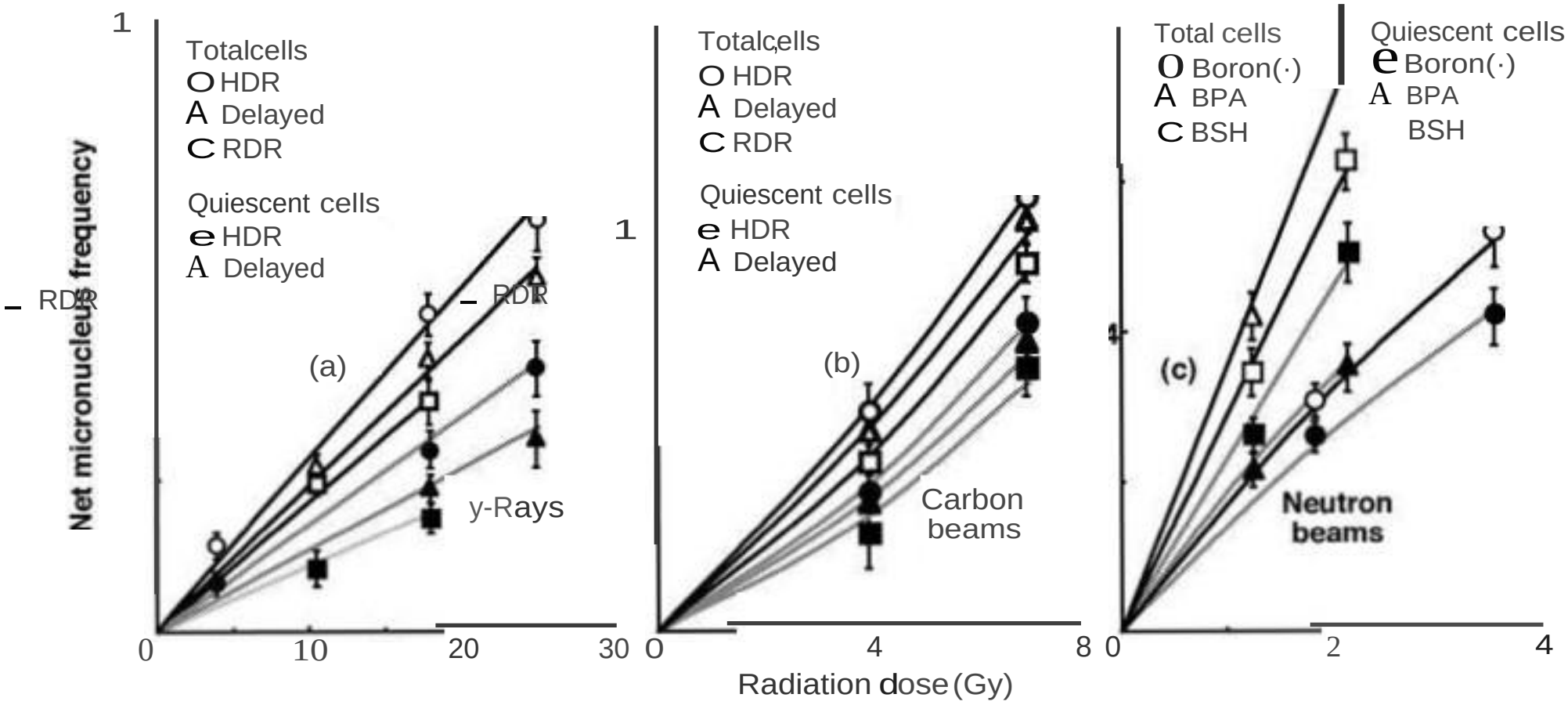

Figure3

Click hereto d<WYnbJd high rtsolution image